ELSEVIER

Catalysis Today 40 (1998) 59–71

CATALYSIS TODAY

Catalytic wet oxidation of acetic acid using platinum on alumina monolith catalyst

Alec A. Klinghoffer[1], Ramon L. Cerro[2], Martin A. Abraham*

Department of Chemical Engineering, The University of Tulsa, Tulsa, OK 74104, USA

Abstract

The aqueous phase oxidation of acetic acid, used as a model compound for the treatment of controlled ecological life support system (CELSS) waste, was carried out in the monolith froth reactor which utilizes two-phase flow in the monolith channels. The catalytic oxidation of acetic acid was carried out over a Pt/Al_2O_3 catalyst at temperatures and pressures below the critical point of water. Multivariable non-linear regression of temperature-dependent data revealed a reaction order of 1.22 ± 0.54 and an activation energy of 89.8 ± 13.4 kJ/mol. Since the reaction order bracketed first-order kinetics, a pseudo-first-order rate constant of $k_1=10^{5.713\pm2.0}\exp[81.04\pm19.0\text{ kJ/mol})/RT]$ was obtained. This value is similar to values reported for the oxidation of acetic acid in other systems and is comparable to intrinsic values calculated for oxidation reactions. Although a recycle reactor was used, separating the effects of fluid mechanics from reactor residence time, the measured rate was dependent on the liquid flow rate. The results were interpreted in terms of detailed flow phenomenon that have previously been determined and reported. © 1998 Elsevier Science B.V.

Keywords: Wet oxidation; Monolith catalyst; Acetic acid; Monolith froth reactor; Waste treatment

1. Introduction

The need for recycle and recovery of usable materials is very important in a controlled ecological life support system (CELSS), defined as a life support system that relies heavily on biological subsystems for recycling [1]. For example, recycled carbon dioxide, water, and inorganic nutrients can be supplied to a crop growth chamber to grow food in a closed environment. There are also several physical/chemical methods currently under investigation for recycling and waste treatment in a CELSS including thermal processes such as incineration, wet air oxidation, and supercritical water oxidation, and non-thermal processes such as electrochemical oxidation and ultraviolet (UV) radiation [2]. One promising and effective method of waste treatment and recycling is wet air oxidation [3].

Wet air oxidation (WAO) is defined as the liquid phase oxidation of organic compounds at temperatures (125–320°C) and pressures (0.5–20 MPa) below the critical point of water using a gaseous source of oxygen [4]. WAO is a well-established technique for the treatment of highly organic and toxic waste water. Pollutant molecules of these various waste streams are oxidized to low molecular weight car-

*Corresponding author. Present address: Department of Chemical and Environmental Engineering, University of Toledo, Toledo,

[1]Present address: Chemical Engineering Department, Texas A & M University, College Station, TX 77843, USA.

[2]Present address: Chemical Engineering Department, University of Alabama in Huntsville, Huntsville, AL 35899, USA.

PII S0920-5861(97)00122-3

boxylic acids, mainly acetic acid, which in turn, are oxidized to carbon dioxide and water if the reaction conditions are severe enough [5–8].

Since it has been observed that the effectiveness of wet air oxidation is limited by the rate of oxidation of low molecular weight carboxylic acids, research on the WAO of low molecular weight acids is of great importance. WAO of several low molecular weight acids including formic, acetic, propionic, butyric, valeric, and caproic acids has been carried out [9–13], as has the oxidation of dicarboxylic acids such as oxalic, adipic, succinic, and glutaric acids. The goal of the studies was to determine reaction orders with respect to reactant and oxygen and the activation energy. Temperatures and pressures of these studies were 112–300°C and 0.35–12.8 MPa, respectively. As a general rule, the oxidation rate increases with an increase in molecular weight of the organic acid.

Since the rate of oxidation of low molecular weight acids is slow, homogeneous and heterogeneous catalysts have been used to increase the rate of oxidation. Homogeneous catalysts are believed to be more effective in increasing the rate of oxidation [14–16] but heterogeneous catalysts are preferred because no catalyst recovery step is required. The heterogeneous catalysts that have been used are Cu, Pd, CoO/ZnO, Cu:Mn:La oxides on spinal supports (ZnO, Al_2O_3), copper chromite, iron oxide, Co:Bi complex oxides, Ru/Ce, and Mn/Ce. Results have shown that the multicomponent catalyst systems (Co:Bi, Cu:Co, Cu:Co:Bi) were the most active catalysts. Imamura et al. [17–19] found that Co:Bi catalyst exhibited the highest activity for the oxidation of acetic acid. They postulated that after acetic acid adsorbed on basic sites, a reduction–oxidation reaction took place between the catalyst and acetic acid, leading to decomposition of the acid. Experiments with carboxylic and dicarboxylic acids reveal that the reaction order with respect to both reactant and oxygen concentration was in the range 1–1.5 [20,21]. The activation energies reported for catalytic WAO were 75–142 kJ/mol for the carboxylic acids.

Previously, three-phase reactions have been carried out in slurry and trickle-bed reactors. In these three-phase reactors, gas and liquid are fed into the reactor separately (as is the case with the slurry reactor) or flowed concurrently down through the bed (trickle-bed reactor). Current reactor designs have the advantage of measuring intrinsic reaction rates and providing good temperature control. However, there are also disadvantages, including costly catalyst recovery steps and slow gas–liquid mass transfer rates in the case of slurry reactors, or channeling of the gas and liquid feeds in the trickle-bed reactor.

Recently, a novel monolith froth reactor, utilizing two-phase bubble-train flow within the channels of the monolith, was developed at The University of Tulsa. The earliest work [22,23] focused on the aqueous-phase catalytic oxidation of phenol over a copper oxide catalyst, during which it was determined that flow characteristics were strongly dependent on gas flow rate and weakly dependent on liquid flow rate. Crynes [24] repeated these experiments at higher temperatures and pressures (150°C, 1.65 MPa), and observed that the reaction rate increased with an increase in temperature, pressure, and phenol concentration, but decreased with an increase in gas flow rate. The reaction rate also exhibited a maximum with respect to liquid flow rate, while conversion decreased with increasing liquid flow rate.

The current paper focuses on the use of a platinum catalyst for the oxidation of acetic acid (CH_3CO_2H). The effects of temperature and liquid flow rate on the acetic acid conversion have been investigated, and are described in terms of the flow behavior now known to exist within the reactor. Power law kinetics is used to assess the performance of the reactor, to explain the results in terms of the theory, and to permit calculation of an activation energy for comparison with literature values.

2. Monolith froth reactor model

Bubble-train flow consists of alternating gas bubbles and liquid slugs within the channels of the monolith, as indicated in Fig. 1(a). This type of flow is characterized by gas bubbles that have a diameter close to the diameter of the channel and a length that is greater than the diameter of the channel. Liquid slugs and gas bubbles pass a fixed point along the monolith channel in succession. The gas bubble has a diameter that is approximately the same size as the monolith channel, thus a very thin liquid film is formed on the surface of the catalyst. In experiments involving bubble-train flow in capillaries, stable liquid films have

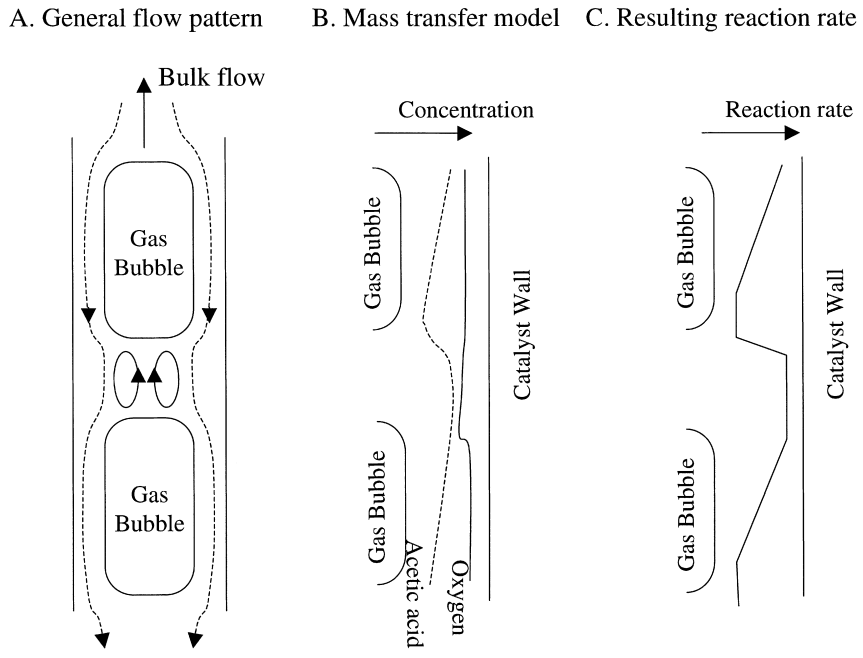

Fig. 1. Schematic description of theoretical models within a single ideal monolith channel: (a) liquid and gas flow patterns; (b) concentration profile for a reacting species; and (c) expected reaction rate.

been generated with thickness less than 10 μm [25]. Although bulk liquid flow is concurrent with the gas flow, liquid in the film alongside the bubble drains downwards due to gravity [26], creating a laminar film flow region along the surface of the catalyst. At the slug, the liquid can either mix with the liquid in the slug, or, depending upon the flow parameters, will undergo complete bypass, as indicated in Fig. 1. As the next gas bubble enters the liquid slug, it further pushes liquid into the film region. The liquid within the slug circulates, and the two liquid flows exchange mass at the boundary between the slug and the film. This process continues as gas bubbles and liquid slugs flow concurrently over the catalyst surface.

Conversion of acetic acid occurs at the catalyst wall through chemical reaction. Following standard analysis, the reaction rate is dependent upon the concentration of the reacting species at the surface. In turn, the rate of mass transfer across the liquid interface controls the concentration of the reactants at the catalyst surface. Because a periodic flow of the gas bubble and the liquid slug pass a single point along the surface of the catalyst, a complex concentration profile develops along the catalyst surface. One possible profile is depicted schematically in Fig. 1(b), and is developed as follows based on our current understanding of fluid flow and mass transfer within the monolith channel.

Mass transfer of reactants to the catalyst is different in the film and liquid slug region [24]. In the film region, oxygen is transferred from the gas–liquid interface through the liquid film. Oxygen is also transferred as the liquid from the slug drains into the film. No convective forces help in transferring oxygen in the radial direction. Mass transfer of oxygen to the catalyst surface is relatively rapid, because the liquid film is very thin. The entire liquid film is in contact with the gas bubble, thus the oxygen concentration is at the equilibrium value along the entire length of the gas bubble. Since the rate of mass transfer is assumed to be relatively high, the concentration of oxygen is approximately equal to the equilibrium concentration of oxygen everywhere within the film.

Crynes [24] states that in the liquid slug region, oxygen is transferred into the liquid phase through the ends of the bubbles in front of and behind the slug.

Oxygen is also transferred to the slug as the liquid film surrounding the preceding bubble drains into the slug. Therefore, mass transfer in this region occurs by convection because of recirculation in the slug. In addition, recirculation of the slug causes the acetic acid concentration to remain uniform within the slug. Thus the acetic acid in the film is regenerated through contact with the liquid slug.

At the top of the liquid film, the acetic acid concentration is approximately equal to the concentration within the preceding slug. Because reaction occurs within the film, acetic acid is depleted along the length of the gas bubble. The film travels in laminar flow, thus the acetic acid is not replenished. If the gas bubble is sufficiently long, acetic acid can be completely depleted from the film region.

Standard reaction kinetics analysis states that the reaction at the surface of the catalyst is dependent upon the concentration of both acetic acid and oxygen. The previous discussion reveals that the oxygen concentration is approximately uniform everywhere along the length of the catalyst surface, whereas the acetic acid is depleted along the bubble and regenerated within the slug region. When translated into an instantaneous reaction rate (at a given point), one should observe a periodic rate profile, depicted as in Fig. 1(c). However, the observed rate of reaction along the entire length of capillary (the "measured" rate) is an average over all unit cells within the capillary. Clearly, an optimum ratio of bubble length to slug length should exist, that depends closely on the ratio of the intrinsic reaction rate to the mass transfer rate.

3. Experimental

Fig. 2 presents a schematic representation of the monolith froth reactor used in this study. The reactor was operated as a recycle reactor. The system may be divided into three smaller systems: feed, reactor, and

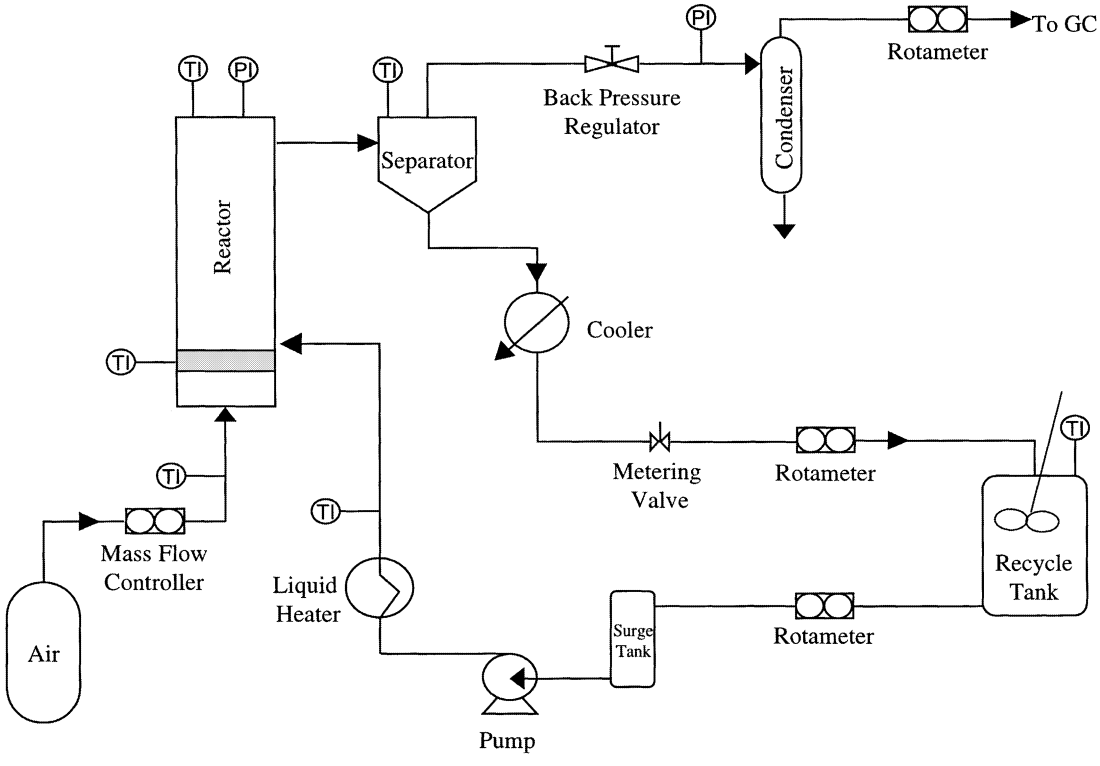

Fig. 2. Schematic diagram of experimental equipment.

separation. The entire reactor system is described in detail elsewhere [27], so it is only discussed briefly in the following paragraphs.

The liquid reaction mixture from a 7.5 l polypropylene recycle tank was drawn by pump suction through a high precision liquid rotameter (Omega model FL-113) into a diaphragm metering pump (Crane Chem/Meter Series 200). The pump was modified to deliver approximately 250 cm^3/min of liquid at a pressure of 13.8 MPa. The liquid was then passed into a heater consisting of three, 10 ft sections of 0.635 cm diameter 316 stainless steel tubing wrapped with high-temperature ceramic bead heaters and insulated to minimize heat loss to the environment. The heater was controlled by feedback from a thermocouple located in the froth section at the inlet of the reactor. Temperature was also monitored at the outlet of the heating unit. After exiting the heater, the liquid was fed from opposite sides into the reactor.

Gas was fed from a high pressure cylinder, through a 40–50 μm filter, and into a mass flow meter (Omega model FMA-871-V). Gas entered the reactor through 0.635 cm 316 stainless steel tubing wrapped with the same type of heating tape used on the liquid feed line. The temperature of the incoming feed gas was monitored by a thermocouple inserted into the gas feed line just prior to the reactor. A Nupro lift type check valve, model SS-5354, was located in the gas feed line to prevent backflow of gas and liquid to the mass flow meter.

Upon entering the reactor, the gas passed up through a glass frit (145–175 μm pore size, 54 mm diameter, 10 mm thick) over which the liquid was dispersed. This resulted in the generation of a ''froth'', a collection of bubbles of uniform dimensions, which entered the channels of the monolith. A thermocouple was located in the frothing region just below the monolith catalyst. This thermocouple measured the temperature of the frothing region and, hence, the inlet reactor temperature. This thermocouple was used to control the liquid heater.

Above the froth region, the reactor was constructed of 5 cm diameter, Schedule 80, 304 stainless steel pipe (ID=4.93 cm, OD=6.04 cm). The reactor length above the gas–liquid distributor was 60 cm. The reactor was wrapped with a heating tape to provide an additional source of heating and was heavily insulated to minimize heat loss to the environment and to provide a constant temperature along the length of the reactor.

Four monolith cores (62 channels/cm^2) were stacked in the reactor to give a total catalyst length of 42.4 cm. The top core was angled 15° from the horizontal to allow liquid to drain from the cores into the separator. The cores were prepared at The University of Tulsa following a procedure described later. The monolith cores were wrapped with Fibrafax, a ceramic fiber insulating paper, 0.16 cm thick, manufactured by The Carborundum company. The wrap expands when wet, creating a tight seal between the cores and the reactor wall. This serves to keep the cores in place and also prevents gas and liquid flow from bypassing the catalyst.

Temperature was monitored above the monolith using a 0.16 cm type K ungrounded thermocouple placed directly above the monolith core; this temperature measurement was used to control the reactor heating rate. The reactor pressure was measured using a pressure transducer (Omega model PX612-3KGV) placed in the gas above the monolith. A 1.748 F, type B, 316 stainless steel rupture disc, rated for 4.14 MPa at 22°C and 3.33 MPa at 250°C, was located at the top of the reactor.

The gas and liquid reaction products flowed out of the reactor into a visual separator (Jerguson size 1-R 20). The liquid level in the separator was manually controlled to maintain a constant level to prevent liquid from flooding out of the top and to avoid surges of gas out of the bottom. Level control was done manually using a sight gauge and a 0.635 cm Hoke Milli-Mite forged micrometering valve, constructed of 316 stainless steel.

The liquid was cooled prior to the micrometering valve to prevent flashing. Upon exiting the cooling unit, the liquid product flowed through a liquid rotameter, similar to one described previously, to measure the exit liquid flow rate and was returned to the recycle tank. Liquid samples were removed from the bottom of the tank through a septum port.

The gas exited from the top of the separator through a back pressure regulator (GO model BP-60), which controlled the reactor pressure. Following the back pressure regulator, the gas was brought to another separator to remove any condensable components from the gas. The gas then flowed through a rotameter (Omega model FL-114) to measure the exit gas flow

rate. The gas was then sent to a gas chromatograph (GC), equipped with an automatic sampling valve, for on-line gas phase analysis.

A plastic shield surrounded the entire reactor system as an additional safety measure. A door in the front of the shield allowed access to the equipment as needed.

3.1. Catalyst description

A platinum catalyst was prepared at The University of Tulsa using the method of incipient wetness. Monolith bricks, 62 channels/cm^2, coated with bare alumina (Al_2O_3) washcoat, were obtained from Allied-Signal. Six monolith cores were cut to the desired specifications (4.4 cm in diameter and 10.9 cm in length) using a 5.1 cm P33F Premium, thin crown diamond core bit, and a drill press. The cores were drilled from the bricks, with extreme care as to insure that the cores were drilled in the direction of the channels. Compressed air was blown through the channels to remove any dust or particles that were trapped as a result of drilling. Two cores were designated as the top cores and angled 15° from the horizontal, as previously described, to allow liquid to drain from the top of the monolith. Partial channels around the monolith were removed to have uniformity of channels along the length of the core.

A solution, 0.5% platinum by weight, was prepared by dissolving 2.626 g of hexachloroplatinate (H_2PtCl_6) into 250.0 g of double-distilled measured water. The solution was stirred using a hot plate and magnetic stir bar until all of the hexachloroplatinate was dissolved. Before impregnation, three monolith cores were dried in a muffle oven at 120°C to remove any atmospheric moisture that might have accumulated on the catalyst washcoat. Following drying, the cores were allowed to air dry for approximately 1 min at room temperature to allow the cores to be weighed. The dry cores were weighed, then dipped into the platinum solution for 5 min. The liquid entered the channels of the monolith by capillary action. The core was then removed from the solution and allowed to ''drip dry'', until no liquid dripped from the channels. The core was turned over and placed back into the solution for 5 min. Again, the monolith was removed from the solution and allowed to ''drip dry'' until no liquid left the channels. All three cores were impregnated in the same manner.

Following impregnation, the cores were placed in the muffle oven to dry at 120°C for 2 h. After 2 h, the oven was shut off and the impregnated cores were allowed to cool off in the oven for approximately 25 min. Following cool down, each core was weighed and placed in a plastic bag to prevent any contamination. The above procedure was repeated for an additional three monolith cores. The six cores were placed in a high temperature furnace to be calcined overnight at 500°C. The cores were placed in the furnace horizontally to promote flow through the channels by convection. After calcination, each core was weighed but showed no appreciable difference in weight before calcination.

Three cores were loaded into the reactor as previously described and used for all kinetic experiments. The total amount of platinum on the three cores in the reactor was 0.9378 g. The amount of platinum on each core was determined by calculating the weight difference of each core before impregnation and after calcination. It was assumed that the weight difference represented the amount of platinum metal on each core.

3.2. Analytical methods

Gas product samples were analyzed on-line using a Hewlett-Packard 5890 gas chromatograph (GC) equipped with an automatic sampling valve and a thermal conductivity detector. The gas products were separated using a 80/100 mesh Porapak N 0.635 cm×304.8 cm stainless steel column with an initial oven temperature held at 50°C for 3 min then ramped to 120°C at a rate of 10°C/min. The detector temperature was 175°C and the sampling valve was heated to 100°C to prevent condensation of water vapor or other condensable products. The GC was calibrated for CO_2 prior to all experiments.

The liquid product was analyzed using a Hewlett-Packard 5890 Series II GC equipped with a flame ionization detector. The liquid product analysis was performed using an SPB-5, 15 m×0.53 mm capillary column. 1.0 μl of sample was manually injected into the GC. The oven temperature was initially maintained at 50°C for 3 min, then ramped to 150°C at 5°C/min. The injector and detector temperatures were

250°C and 260°C, respectively. A calibration curve was constructed before every analysis by preparing and analyzing standards in the range of product acetic acid concentration.

The liquid product and liquid feed samples were also analyzed for platinum using a Perkin-Elmer 603 atomic absorption spectrophotometer (AAS) equipped with a graphite furnace. The Pt hollow cathode lamp was operated at 10 mA and the AAS was operated in the absorbance mode. Three standard solutions were prepared from a 980 ppm (w/w) reference standard to calibrate the instrument. Water purified with a Milli-Q system (Millipore) was used to dilute the reference sample and as a blank between each sample. Each standard was injected into the AAS three times and the average absorbance was recorded. Blanks consisting of the purified water were run between each standard. Absorbance as a function of concentration was recorded and fit to a straight line using linear regression. A representative sample from each experiment was analyzed. This representative sample was usually the final sample taken from the recycle tank during a run. This should coincide with the maximum amount of platinum that would be lost from the catalyst during the course of an experiment. Each sample was then analyzed three times using the above-mentioned procedure and the average absorbance was recorded. The average concentration of platinum in the solution was calculated using the calibration curve. The weight of platinum in solution during each experiment was calculated by the following equation:

$$\frac{\text{weight of platinum } (\mu\text{g})}{7000\,\text{cm}^3 \text{ of } H_2O} \times 10^6 = [\text{concentration of platinum}]\,\text{ppm}.$$

4. Results

The complete catalytic oxidation of acetic acid can be described by the following equation:

$$CH_3CO_2H + 2O_2 \rightarrow 2CO_2 + 2H_2O \quad (1)$$

The only reaction product detected from the monolith froth reactor was CO_2. No partial oxidation products of acetic acid (formic and oxalic acid or formaldehyde) were detected in this study. No carbon monoxide was detected during the course of this study, indicating that the catalyst maintained its activity for the duration of the study. These results are consistent with those of previous researchers, who have investigated the oxidation of acetic acid [17,18,21]. Levec and Smith [22] used a trickle-bed reactor operating in downflow mode, with a ferric oxide catalyst and observed no gas-phase acetic acid or carbon monoxide or liquid-phase formic acid or formaldehyde.

The monolith froth reactor was operated as a recycle reactor and all data are reported in the form of conversion as a function of run time. The amount of acetic acid remaining in the recycle tank was determined using HPLC and GC analysis of the liquid. A mass balance on acetic acid reveals that since the entire reactor system is closed, the rate of reaction (integrated over the entire volume of the system) is identically equal to the rate of disappearance of acetic acid,

$$\int^{V} r_A \, dV = \frac{dN_A}{dt}. \quad (2)$$

If we express the reaction rate as an average value over the entire system, and note that the volume of the system remains constant, we obtain

$$r_A = \frac{dC_A}{dt}, \quad (3)$$

the standard batch reactor design equation.

As an alternative to using the volume as the measure of total quantity, one might wish to express the rate in terms of the catalyst mass. This is easily accomplished using a variable conversion,

$$r'_A = \frac{V}{W}\frac{dC_A}{dt}, \quad (4)$$

where V represents the total volume of liquid and W is the catalyst weight. Eqs. (3) and (4) differ simply by the ratio V/W, which was maintained constant in all experimental runs.

4.1. Effect of temperature

The effect of temperature on reactor performance is indicated in Fig. 3 as a plot of conversion vs. run time. The data were recorded at three temperatures (200°C, 220°C, and 240°C) and an initial recycle tank concentration of 0.0554 mol/l. The liquid flow rate for all

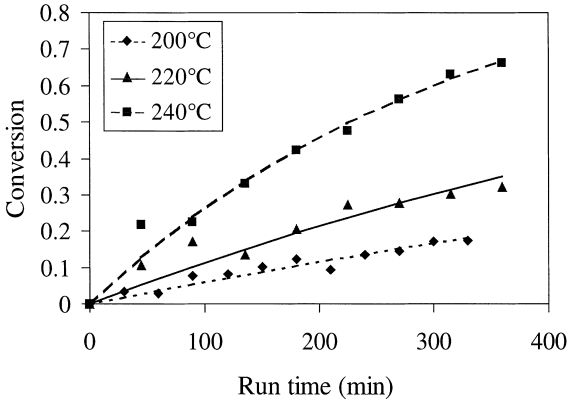

Fig. 3. Temporal variation of acetic acid conversion as a function of reactor temperature. Curves represent prediction of first-order model.

three data sets was 62 cm^3/min and the gas flow rate was 2750 N cm^3/min. All experiments were performed at a constant volumetric gas flow rate as measured by the mass flow meter. These flow rates were chosen because they provided the best temperature control and best overall operation of the system. As shown in Fig. 3, increasing temperature led to an increase in conversion, as expected.

The experimental data are correlated using power law kinetics,

$$r_A = \frac{dC_A}{dt} = -(Ae^{-E/RT})C_A^n, \quad (5)$$

where the rate constant is replaced by the usual Arrhenius dependence on temperature. As described by the monolith model, the oxygen concentration was approximately constant within the liquid film, and since air was used in all experiments, this term could be lumped together with the rate constant to provide an apparent rate constant. Solving Eq. (5) for concentration as a function of time, we get

$$C_A = [C_{A,0}^{1-n} - (1-n)(Ae^{-E/RT})t]^{1/(1-n)}. \quad (6)$$

Although this equation is highly non-linear, it was possible to perform a multivariable non-linear regression to determine an overall reaction order of 1.22±0.54 and activation energy of 89.8±13.4 kJ/mol. One may also fit the concentration vs. time data to a polynomial and then differentiate the polynomial with respect to time, to obtain data in the form of rate vs. concentration. Following these data conversions, multivariable linear regression may be completed by transforming Eq. (5) into a linear form,

$$\ln\left(-\frac{dC_A}{dt}\right) = \ln A - \frac{E}{RT} + n \ln C_A. \quad (7)$$

Using this analysis, the overall reaction order was determined to be 0.84±0.54, with an activation energy of 76.9±18.0 kJ/mol and frequency factor of $10^{5.04\pm2.47}$ $(mol/l)^{0.16}$ min^{-1}.

In neither of the multivariable regression were the reaction order statistically different from the other, thus pseudo-first-order rate constants were also obtained; the resulting values are indicated for all experimental runs in Table 1. The conversion predicted by the first-order model is compared with the experimental data and shown as the solid lines in Fig. 3. The values of the first-order rate constants are plotted in Arrhenius form in Fig. 4. From the linear regression of this pseudo-first-order data, the activation energy was calculated as 81.04±19.0 kJ/mol with a frequency factor of $10^{5.71\pm2.0}$ min^{-1}.

Table 1
Estimated first-order rate constants

Temperature (°C)	Flow rate (cm^3/min)	k (min^{-1})
200	57.76	0.00061±0.00005
220	62.59	0.0012±0.00016
220	28.47	0.0018±0.00021
220	107.44	0.0014±0.00024
240	62.47	0.0031±0.00016

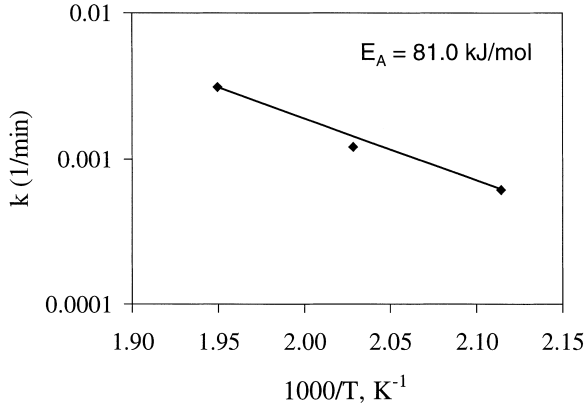

Fig. 4. Temperature dependence of the pseudo-first-order rate constant.

It is reassuring to note that three entirely different methods of estimating the values of the rate parameters provided statistically consistent results, providing a high degree of confidence in these calculations. In addition, the values of the rate parameters are consistent with the results of previous researchers investigating the oxidation of acetic acid. Levec and Smith [21], studying the oxidation of acetic acid using a ferric oxide catalyst in a trickle-bed reactor, reported that the reaction was first-order in acetic acid concentration, with an activation energy of 87.9 kJ/mol. This result suggests, as also observed by previous researchers [24], that the observed rate in the monolith froth reactor is close to the intrinsic kinetic rate and is only slightly inhibited by mass transfer.

The reactor pressure was increased as the temperature was increased to prevent excessive vaporization of the liquid. For temperatures 200°C and 220°C, the reactor pressure was twice the vapor pressure of water at those temperatures, and, for 240°C, the reactor pressure was 1.5 times the vapor pressure of water at 240°C. These pressures were chosen so that most of the water remained in the liquid state while remaining within the pressure limits of the system. A single pressure was not used over the entire range of temperatures because a pressure large enough to prevent vaporization at high temperatures would result in a pressure that would cause very small froth bubbles at low temperatures [24]. Although the effect of reactor pressure on conversion of acetic acid and reaction rate was not examined explicitly, there is evidence that it will affect the conversion of acetic acid and reaction rate. The equilibrium concentration of oxygen in the liquid is a function of total pressure. One would then expect the conversion and reaction rate to increase due to the greater availability of oxygen in the liquid phase. Indeed, Crynes [24], investigating the oxidation of phenol in the monolith froth reactor, reported an increase in conversion and reaction rate with an increase in reactor pressure.

It is interesting to note, though, that an increase in temperature would have an opposite effect on the solubility relative to an increase in pressure. As the temperature is increased, the solubility of a gas in a liquid is decreased. The decrease in oxygen concentration in the liquid would cause a decrease in the availability of oxygen in the liquid phase. Therefore, it would be expected that the conversion and reaction rate would decrease. However, this is not found in the results. Unfortunately, it is very difficult to decouple the effects of temperature and pressure on the conversion and reaction rate because the effects are interrelated. Apparently, the effect of an increase in temperature (Arrhenius expression) and pressure (increased solubility of oxygen) outweigh any effect due to the decrease in solubility caused by the increase in temperature because results indicate the conversion and reaction rate increase with an increase in temperature and pressure.

4.2. *Effect of liquid flow rate*

Fig. 5 illustrates the effect of liquid flow rate on the oxidation of acetic acid at 220°C and three liquid flow rates, 28.47, 62.59, and 107.44 cm^3/min, respectively. The gas flow rate was 2700 N cm^3/min. Theoretical calculations indicate that all of these flow rates should provide bubble-train flow within the monolith channels. The initial concentration of acetic acid in the recycle tank was 0.0554 mol/l. As before, the curves represent the conversion predicted by the first-order model, with the rate constants reported in Table 1.

As the liquid flow rate was increased from 28.47 to 62.59 cm^3/min, the acetic acid conversion decreased. However, further increasing the liquid flow rate to 107.44 cm^3/min led to an increase in conversion relative to the data recorded at 62.59 cm^3/min. From a purely macroscopic viewpoint, the liquid residence time in the reactor (time the reactant is in contact with the catalyst) should remain constant regardless of flow

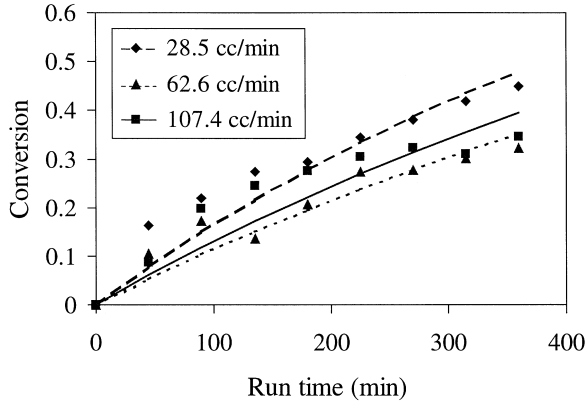

Fig. 5. Temporal variation of acetic acid conversion as a function of liquid flow rate. Curves represent prediction of first-order model.

rate because, as the liquid flow rate increases, the number of cycles of the tank also increases. Therefore, the liquid would be in contact with the catalyst for the same total amount of time in a closed system. Then the liquid flow rate should not affect the conversion of acetic acid.

Since the liquid flow rate does not affect the residence time in the reactor, it must affect the flow characteristics within the channels of the monolith and the characteristics of the froth. The flow regime inside the channels of the monolith is a function of the gas and liquid velocities within the channel. We now note that two-phase flow within the channels can fall into at least three regimes: bubble flow, bubble-train flow, and annular flow. Transition regions can exist between each regime where the flow characteristics fall somewhere between the ideal situation for each regime. At low liquid and high gas flow rates, it is possible that annular flow develops within the channels. In annular flow, the gas phase is continuous and surrounded by a liquid film. Although a liquid film is developed along the catalyst wall, this film is substantially larger than the film that is produced during bubble-train flow. In addition, poor mixing of the film occurs, resulting in poor redistribution of the acetic acid in the liquid film. Thus, annular flow provides poor reactor performance.

Even within the bubble-train flow regime, bubble size, liquid slug size, and liquid film thickness can vary, affecting mass transfer properties and reactor performance. For example, if one increases the liquid flow rate, the Reynolds number would increase, thereby increasing the mass transfer coefficient. Also, froth characteristics and entrance effects can become more pronounced when liquid flow rate is varied. These factors become increasingly important in determining the extent and nature of the bubble-train flow inside the monolith channels.

Thulasidas et al. [25] have observed that the size of the liquid slugs become larger with an increase in liquid flow rate. Recall the concentration profile and possible reaction rate profile shown in Fig. 1. For small bubbles, the average concentration of acetic acid in the film will be close to that of the bulk concentration in the liquid slug. As the bubbles become larger, the average acetic acid concentration decreases. Also, smaller bubbles yield a larger number of unit cells (bubble–slug pairs) within each monolith channel. In addition, larger liquid slugs have more recirculation and axial mixing within the liquid slug. This leads to greater replenishment of acetic acid and oxygen near the surface of the catalyst and higher overall reaction rates. As a result, small bubbles and large liquid slugs should promote high conversion.

4.3. Material balance

The carbon mole balance closure was checked using the stoichiometry of Eq. (1). The total amount of CO_2 produced during the experiment was calculated by summation over the individual CO_2 measurements at each data point. This calculation assumes that the CO_2 concentration is constant during the time interval and equivalent to the concentration at the end of the interval. The amount of acetic acid at the beginning and the end of the experiment could easily be calculated from the measured acetic acid concentration. Combining these concepts leads to Eq. (8). Note that two moles of CO_2 are produced for each mole of acetic acid that reacts:

$$\text{Carbon balance}\,(\%) = \frac{\left(\sum G_i y_{\mathrm{CO}_2,i}\Delta t\right)/2 + C_{\mathrm{AA,f}}V}{C_{\mathrm{AA,i}}V} \times 100\%. \quad (8)$$

Carbon balances ranged from a low of 57% to a high of 93%. The balances were based on the total amount of acetic acid reacted during the course of the experiment and the measured amount of CO_2 produced for the duration of each experiment. No partial oxidation products were detected using GC, liquid chromatography (LC), and FT-IR during the course of the study. No gas phase acetic acid was detected during any experiment.

At elevated pressure, a substantial concentration of carbon dioxide can exist in the liquid phase, either in the form of soluble carbon dioxide, or as carbonate ion. Most of the dissolved carbon would vaporize following the pressure letdown and not be included in the above measurement. An attempt was made to measure the carbonate ion concentration in the liquid samples, however, the technique was unsuccessful because acetic acid interfered with the response of the electrode. It is possible, however, to estimate the dissolved carbon dioxide and carbonate ion concentration using equilibrium thermodynamics. Values of

the equilibrium constants were obtained [28] and indicate that less than 2% of the CO_2 produced would escape with the liquid stream. Thus, the dissolved carbon dioxide does not represent a significant addition to the carbon balance.

Clearly, closure of the material balance is of great concern not only from an experimental point of view but also from the point of view of evaluating wet air oxidation as a viable technology for the removal of CELSS waste. One of the major requirements of a CELSS waste treatment system is to use all of the by-products of the treatment system. For example, CO_2 is recovered and used as a food source for plant growth. Therefore, it is necessary to be able to recover and reuse all materials in a CELSS treatment system. In the current work, it is likely that the failure to close a carbon balance is a result of the estimation techniques for CO_2 production, rather than the formation of undetected products.

4.4. Catalyst stability

The issue of catalyst stability is an important issue for a waste treatment process. For wet air oxidation to be competitive with other treatment processes, the catalyst must not deactivate under severe reaction conditions, retaining its activity for extended periods of time. Since large amounts of water are being treated, there is concern that the active metal on the catalyst will dissolve into the liquid solution, thereby reducing catalyst activity through loss of metal sites. Catalyst stability concerns were raised in the previous study investigating the oxidation of phenol over a copper oxide supported on γ-alumina catalyst [24]. Results indicated that the rate of copper loss appeared to increase with an increase in temperature, pressure, and gas or liquid flow rate. Crynes [24] estimated that approximately 20% of the initial copper loading was lost after 50 h of run time.

To address the issue of catalyst stability, a liquid sample was taken from the recycle tank at the conclusion of each experiment. The final tank material was chosen since this should have the highest concentration of dissolved platinum. Samples were analyzed for Pt metal using a Perkin-Elmer 603 Atomic Absorption Spectrophotometer equipped with a graphite furnace. The detection limit for platinum, as reported by the manufacturer, was 0.03 ppm (w/w). Each sample was analyzed and the amount of platinum that had leached into solution was calculated from this measurement. The total amount of platinum lost during all experiments was calculated by summing the individual amounts of platinum in each solution and comparing this number to the initial amount of platinum impregnated on the catalyst. Experiments that were terminated before completion or experiments that were not used in this study were not included in this calculation. Results indicate that the largest amount of platinum in any one sample was 0.09 ppm (w/w). The total amount of platinum lost, calculated from atomic absorption measurements, was 4.61×10^{-6} g, while the total amount of platinum impregnated on the catalyst was 0.938 g. The amount of platinum that leached into solution was less than 0.01% of the initial loading. Therefore, the catalyst prepared at The University of Tulsa for this study was stable at the reaction conditions tested and for the duration of the study.

5. Scale-up and design issues

One of the major goals of any reactor design or reaction rate study is to use the intrinsic reaction rate data obtained at the bench scale in the design and operation of a commercial scale system. This is important because it is not feasible, from a practical as well as economic viewpoint, to build a large-scale unit and test all possible scenarios. Another important concept, especially for waste treatment applications, is the concept of the design-limiting compound. The design-limiting compound is defined as the compound that is most difficult to destroy (oxidize). The basic idea is that if the system is designed and operated at conditions where the design-limiting compound is destroyed, then the system should be able to effectively destroy all other compounds. These two basic ideas were applied in this study.

The current study focused on wet air oxidation as a method of waste treatment in CELSS. Acetic acid was chosen as the model compound because it has been observed as a stable end product of oxidation from numerous waste streams (municipal sewage sludge, alcohol distillery waste, and effluent streams from pulp and paper mills). Also, acetic acid has been found to have a slow rate of oxidation [4]. Therefore,

the complete oxidation of acetic acid presents a major limitation to the wet air oxidation process.

Many waste treatment applications require very high levels of destruction of the pollutant molecules to such benign species as CO_2 and water. For CELSS waste treatment, a process needs to be able to achieve destruction levels that approach 100% to be a suitable process [29] because the water has to be reused by living organisms. Any system deemed suitable for CELSS waste treatment would have to meet or exceed these levels of destruction.

The first step in verifying that the monolith froth reactor is suitable for CELSS waste treatment is to measure reaction rates for the oxidation of acetic acid. Using the available data (first-order reaction rate constant measured at 240°C), the time required to achieve 99.99% conversion is over 3000 h. This length of processing time is too long to be of practical interest. Therefore, there is a need to increase the reaction rate using available parameters. One obvious way to do this would be to increase the reaction temperature. Since no data were measured above 240°C, the reaction rate constant must be extrapolated using the Arrhenius expression. Unfortunately, this could lead to erroneous results because the true reaction rate might be smaller than the calculated reaction rate if external mass transfer resistance would become important at elevated temperatures.

The current rate expression was written on the basis of total volume. However, if one increases the amount of catalyst in the reactor, then the rate (based on volume) would increase (although the rate based on catalyst weight would remain unchanged). That is,

$$r_A = \frac{W}{V} k' C_A, \tag{9}$$

where k' represents the value of the first-order rate constant expressed on the basis of catalyst weight. In a similar fashion, one could also decrease the total liquid volume in the system, maintaining the same catalyst weight and liquid flow rate. This would also result in a more rapid depletion of the acetic acid in the system, as the number of tank turnovers would be greater for the same length of run time. Clearly, there are several different variables that can be adjusted to achieve the desired level of conversion.

As previously discussed, the monolith froth reactor utilizes bubble-train flow within the channels of the monolith to reduce mass transfer resistance and produce reaction rates that are near intrinsic values. The key to achieving bubble-train flow in the channels is the ''froth'' feed that is generated at the entrance of the monolith. The ''froth'' can be described as a collection of bubbles of differing sizes dispersed randomly in a liquid phase. If the characteristics of the ''froth'' could be described, quantified, and related to reactor performance, the feed system could then be designed to give the optimal reaction conditions. Previous researchers have investigated certain fundamental aspects of the ''froth'' (bubble size distribution) and how a single bubble enters a single capillary, but no work has been done on relating the generation of the ''froth'' to reactor performance.

6. Summary

In comparison to other published literature on the oxidation of acetic acid, the monolith froth reactor appears to compare very favorably. For example, Levec and Smith [21] reported 10–20% conversion of acetic acid using a trickle-bed reactor with a ferric oxide catalyst for temperatures between 250°C and 286°C. Imamura et al. [30] reported a total organic carbon removal of 67% at a temperature of 248°C using Co:Bi (5:1) complex oxides as the catalyst. Imamura et al. [19] also reported total organic carbon removal of 19.4% at a temperature of 200°C using Ru/Ce, $Cu(NO_3)_2$, and Mn/Ce catalysts in a batch reactor. The monolith froth reactor also utilizes the added advantages of the monolith catalyst (lower pressure drop, high surface area to volume ratio, excellent mechanical stability) for the oxidation of acetic acid. However, control of operating parameters such as liquid flow rate must be exercised to achieve optimum performance of the reactor.

Now that such issues as acetic acid destruction and catalyst stability have been addressed, the monolith froth reactor, used as part of a wet air oxidation system, compares favorably with other forms of treatment methods for CELSS wastes. The main advantage of wet air oxidation is that it requires much less energy to operate than incineration because lower temperatures are required for the reaction. The effluent water does not require substantial cooling or post-treatment for partial oxidation products. Also, there is not much

water loss due to evaporation. With the drawbacks addressed and the many advantages presented here, wet air oxidation should be recognized as a viable alternative for waste treatment.

Acknowledgements

This research was supported by NASA Ames Research Center, under Joint Research Interchange NCC2-5151. The authors are grateful to NASA, and in particular, Mr. John Fisher, Lead Engineer of the Regenerative Life Support Group, for support of this research effort.

References

[1] T. Wydeven, J. Tremor, C. Koo, R. Jacquez, ''Sources and Processing of CELSS Wastes'', Advances in Space Research 9 (1989) 85–97.
[2] T. Wydeven, R.S. Upadhye, K. Wignarajah, Incineration for resource recovery in a closed ecological life support system, Environ. Int. 19 (1993) 381–392.
[3] M. Oguchi, K. Nitta, Evaluation of catalysts for wet oxidation management in CELSS, Adv. Space Res. 12 (1992) 521–527.
[4] V.S. Mishra, V.V. Mahajani, J.B. Joshi, Wet Air Oxidation, Ind. Eng. Chem. Res. 34 (1995) 2–48.
[5] S. Imamura, Y. Tonomura, M. Terada, T. Kitao, Oxidation of oxygen containing organic compounds in water, Mizu Shori Gijutsu 20 (1979) 317–321.
[6] S. Imamura, J. Shimai, T. Kitao, Wet oxidation of dyes, Mizu Shori Gijutsu 21 (1980) 109.
[7] S. Imamura, M. Fukuhara, T. Kitao, Wet oxidation of amides, J. Chem. Soc. Jpn. (1980) 270–276.
[8] S. Imamura, Y. Tonomura, N. Kawabatu, T. Kitao, Wet oxidation of water soluble polymers, Bull. Chem. Soc. Jpn. 54 (1981) 1548–1553.
[9] C.R. Bailloud, B.M. Faith, O. Masi, Fate of specific pollutants during wet oxidation and ozonation, Environ. Prog. 1 (1982) 217–227.
[10] C.R. Bailloud, R.A. Lamparter, B.A. Barna, Wet oxidation for industrial waste treatment, Chem. Eng. Prog. (1985) 52–56.
[11] J.W. Fisher, Oxidation of sewage with air at elevated temperatures, Water Res. 5 (1971) 187.
[12] J.N. Foussard, H. Debellefontaine, V.J. Besombes, Efficient elimination of organic wastes: Wet air oxidation, J. Environ. Eng. 115 (1989) 367–385.
[13] A.A. Friedman, J.E. Smith, J. Desantis, T. Ptak, R. Ganley, Characteristics of residue from wet air oxidation of anaerobic sludges, J. Water Pollut. Control Fed. 60 (1988) 1971.
[14] Y. Tagashira, H. Takagi, K. Inagaki, Wet-high pressure wastewater treatment in the presence of copper, Jpn. Kokai Tokkyo Koho JP 75106862, 1975.
[15] S. Goto, J. Levec, J.M. Smith, Trickle bed oxidation reactors, Catal. Rev. Sci. Eng. 15 (1977) 187–267.
[16] S. Imamura, T. Sakai, T. Ikuyama, Wet oxidation of acetic acid catalyzed by copper salts, Sekiyu Gakkaishi 25 (1982) 74–80.
[17] S. Imamura, A. Hirano, N. Kawabata, Wet oxidation of acetic acid catalyzed by Co–Bi complex oxides, Ind. Eng. Chem. Prod. Res. Dev. 21 (1982) 570–575.
[18] S. Imamura, H. Kinunaka, N. Kawabata, The wet oxidation of organic compounds catalyzed by Co–Bi complex oxides, Bull. Chem. Soc. Jpn. 55 (1982) 3679–3680.
[19] S. Imamura, I. Fukuda, S. Ishida, Wet oxidation catalyzed by ruthenium supported on Cerium (IV) oxides, Ind. Eng. Chem. Res. 27 (1988) 718–721.
[20] G. Baldi, S. Goto, C.K. Chow, J.M. Smith, Catalytic oxidation of formic acid in water-intraparticle diffusion in liquid filled pores, Ind. Eng. Chem. Process Des. Dev. 13 (1974) 447–452.
[21] J. Levec, J.M. Smith, Oxidation of acetic acid solutions in a trickle-bed reactor, AIChE J. 22 (1976) 919–920.
[22] S. Kim, Three-phase catalytic oxidation of phenol in a monolithic reactor, M.S. Thesis, University of Tulsa, Tulsa, OK, 1991.
[23] S. Kim, Y. Shah, R. Cerro, M. Abraham, Aqueous phase oxidation of phenol in a monolithic reactor, AIChE Second Topical Pollution Prevention Conference Preprints, Pittsburgh, PA, 20–21 August, 1991.
[24] L.L. Crynes, Development of a novel monolith froth reactor for three-phase catalytic reactions, Ph.D. Dissertation, University of Tulsa, Tulsa, OK, USA, 1993.
[25] T.C. Thulasidas, M.A. Abraham, R.L. Cerro, Bubble-train flow in capillaries of circular and square cross section, Chem. Eng. Sci. 50 (1995) 183.
[26] W. Kolb, The coating of monolith structures: Analysis of flow phenomena, Ph.D. Dissertation, University of Tulsa, Tulsa, OK, USA, 1993.
[27] A.A. Klinghoffer, Aqueous phase oxidation of acetic acid using a platinum monolith catalyst, M.S. Thesis, University of Tulsa, Tulsa, OK, 1997.
[28] W. Stumm, J.J. Morgan, Aquatic Chemistry, Wiley, New York, 1994, p. 981.
[29] Y. Takahashi, T. Wydeven, C. Koo, ''Subcritical and Supercritical Water Oxidation of CELSS Wastes'', Advances in Space Research 9 (1989) 99–110.
[30] S. Inamura, M. Nakamura, N. Kawabata, J. Yoshida, S. Ishida, ''Wet Oxidation of Poly(ethylene glycol) Catalyzed by Manganese-Cerium Composite Oxide'', Ind. Eng. Chem. Prod. Res. Dev. 25 (1986) 34–37.